Synthesis, Structure, and Reactivity of Heterometallic Polyhydride Complexes of Rhenium with Yttrium and Lutetium

Daniel Alvarez, Jr.,[†] Kenneth G. Caulton,*[,†] William J. Evans,*[,‡] and Joseph W. Ziller[‡]

Departments of Chemistry, Indiana University, Bloomington, Indiana 47405, and University of California at Irvine, Irvine, California 92717

Received June 4, 1992

Yttrium and lutetium methyl complexes readily react with rhenium hydride compounds to eliminate methane and form heterometallic polyhydride complexes. The complexes $(C_5H_5)_2LnMe(THF)$ (Ln = Y, Lu) react with $ReH_7(PPh_3)_2$ and $ReH_5(PMe_2Ph)_3$ to form $(C_5H_5)_2Ln(THF)H_6Re(PPh_3)_2$ and $(C_5H_5)_2Ln(THF)H_4Re(PMe_2Ph)_3$. $(C_5H_5)_2Y(THF)H_6Re(PPh_3)_2$, **1**, crystallizes from 3:1 toluene/THF at −35 °C in space group $P2_1/c$ (C_{2h}^5; No. 14) with a = 19.886 (4) Å, b = 9.8014 (15) Å, c = 25.815 (5) Å, β = 102.653 (15)°, V = 4909.5 (15) Å^3, and D_{calcd} = 1.49 g cm^{-3} for Z = 4. Least-squares refinement of the model based on 5022 reflections ($F^2 > 3.0\sigma(F^2)$) converged to a final R_F = 5.0%. $(C_5H_5)_2Y(THF)H_4Re(PMe_2Ph)_3$, **2**, crystallizes from hexane at −35 °C in space group $Pca2_1$ (C_{2v}^5; No. 29) with a = 21.537 (4) Å, b = 11.734 (2) Å, c = 30.142 (4) Å, V = 7617 (2) Å^3, and D_{calcd} = 1.562 g cm^{-3} for Z = 8. Least-squares refinement of the model based on 5087 reflections ($F^2 > 4.0\sigma(F^2)$) converged to a final R_F = 5.8%. Both **1** and **2** exist as molecular species containing bridging hydride ligands. In each case, the geometry around each metal resembles that in analogous monometallic systems with some distortions arising from steric crowding. The complexes $(C_5H_5)_2LnMe(THF)$ (Ln = Y, Lu) also react with $Re_2H_8(PMe_2Ph)_4$ in THF to form $(C_5H_5)_2Y(THF)H_7Re_2(PMe_2Ph)_4$, **3**, and $(C_5H_5)_2LuH_7Re_2(PMe_2Ph)_4$, **4**. **3** crystallizes from hexane at −35 °C in space group $P2_1/n$ with unit cell parameters at 213 K of a = 11.9546 (16) Å, b = 31.613 (4) Å, c = 12.571 (2) Å, β = 92.376 (11)°, V = 4746.5 (11) Å^3, and D_{calcd} = 1.712 g cm^{-3} for Z = 4. Least-squares refinement of the model based on 6616 reflections ($F^2 > 4.0\sigma(F^2)$) converged to a final R_F = 6.1%. **4** crystallizes from hexane at −35 °C in space group $P2_1/c$ with unit cell parameters at 183 K of a = 16.677 (4) Å, b = 12.960 (2) Å, c = 19.199 (3) Å, β = 90.990 (16)°, V = 4397.7 (14) Å^3, and D_{calcd} = 1.87 g cm^{-3} for Z = 4. Least-squares refinement of the model based on 4253 reflections ($F^2 > 3.0\sigma(F^2)$) converged to a final R_F = 4.9%. Complex **3** is a fluxional molecule which contains an open L-shaped YRe_2 unit. Complex **4** contains a closed triangular $LuRe_2$ core which will not add THF. THF can be removed from **3** to form an yttrium analog of **4**. The bimetallic complex **1** is unreactive toward CO, CO_2, and PhC≡CPh but is highly reactive toward olefin polymerization. In contrast, the trimetallic complexes $(C_5H_5)_2LnH_7Re_2(PMe_2Ph)_4$ are reactive toward CO and CO_2 but unreactive with ethylene.

Introduction

In recent years, considerable effort has been devoted to the synthesis of mixed-metal complexes containing significantly different types of metals.[1,2] With two or more disparate metal centers in a single molecule, the potential exists for cooperative behavior which will permit reaction chemistry which cannot be accessed by either metal individually. Initial syntheses of mixed-metal complexes necessarily employed stabilizing ligands on each metal along with strongly bridging ligands to bind the two metals together.

A particularly challenging aspect of the further development of heterometallic chemistry is the synthesis of mixed-metal complexes which contain reactive ligands. Hydride ligands are highly desirable for this purpose. They not only have the capacity to bridge a variety of different elements but they are also sites of reactivity. In addition, they have minimal steric and orbital requirements and hence can be accommodated in a variety of metallic coordination environments.

We report here on our efforts to generate mixed-metal polyhydride complexes using rhenium polyhydride phosphines and cyclopentadienylyttrium and -lanthanide alkyl complexes as precursors. Bimetallic alkane elimination reactions involving Bronsted acidic transition metal hydrides (eq 1) have been known

$$M\text{–}Me + M'\text{–}H \rightarrow CH_4 + M\text{–}M' \qquad (1)$$

for years,[3] and our preliminary studies[2] showed that they were also useful for coupling yttrium to less acidic rhenium phosphine complexes.[2] It now appears that this is a generally applicable route to heterometallic hydrides of these metals. Four structural types of mixed-metal complexes are reported here along with preliminary patterns of reactivity for these heterometallic species.

Experimental Section

Manipulations of the complexes described below were conducted with the rigorous exclusion of air and water with Schlenk, vacuum line, and glovebox techniques. Solvents were purified and physical measurements were obtained as previously described.[4] $ReH_7(PPh_3)_2$,[5,6] $ReH_5(PMe_2Ph)_3$,[6-8] $ReH_5(PPh_3)_3$,[6-8] $Re_2H_8(PMe_2Ph)_4$,[6] and $Cp_2LnMe(THF)$ (Cp = C_5H_5; Ln = Y, Lu)[9] were prepared by literature

† Indiana University.
‡ University of California at Irvine.

(1) Roberts, D. A.; Geoffroy, G. L. In *Comprehensive Organometallic Chemistry*; Wilkinson, G., Stone, F. G. A., Abel, E. W., Eds.; Pergamon Press: Oxford, England, 1982; Vol. 6, Chapter 40 and references therein.
(2) Alvarez, D., Jr.; Caulton, K. G.; Evans, W. J.; Ziller, J. W. *J. Am. Chem. Soc.* **1990**, *112*, 5674–5676 and references therein.
(3) (a) Hoxmeier, R.; Deubzer, B.; Kaesz, H. D. *J. Am. Chem. Soc.* **1971**, *93*, 536–537. (b) Renault, P.; Tainturier, G.; Gautheron, B. *J. Organomet. Chem.* **1978**, *150*, C9–C10. (c) Marsella, J. A.; Huffman, J. C.; Caulton, K. G.; Longato, B.; Norton, J. R. *J. Am. Chem. Soc.* **1982**, *104*, 6360–6368. (d) Longato, B.; Martin, B. D.; Norton, J. R.; Andersen, O. P. *Inorg. Chem.* **1985**, *24*, 1389–1394. (e) Edidin, R. T.; Sullivan, J. M.; Norton, J. R. *J. Am. Chem. Soc.* **1987**, *109*, 3945–3953.
(4) (a) Evans, W. J.; Chamberlain, L. R.; Ulibarri, T. A.; Ziller, J. W. *J. Am. Chem. Soc.* **1988**, *110*, 6423–6432. (b) Vaartstra, B. A.; Huffman, J. C.; Streib, W. E.; Caulton, K. G. *Inorg. Chem.* **1991**, *30*, 121–125.
(5) Cameron, C. J.; Moehring, G. A.; Walton, R. A. *Inorg. Synth.* **1990**, *27*, 14.
(6) Chatt, J.; Coffey, R. S. *J. Chem. Soc. A* **1969**, 1963–1972.
(7) Ginsberg, A. P.; Abrahams, S. C.; Jameison, P. B. *J. Am. Chem. Soc.* **1973**, *95*, 4751.
(8) Teller, R. G.; Carroll, W. E.; Bau, R. *Inorg. Chim. Acta* **1984**, *87*, 121–127.

0020-1669/92/1331-5500$03.00/0

Table I. Crystal Data and Summary of Intensity Data Collection and Structure Refinement for $Cp_2Y(THF)H_6Re(PPh_3)_2$ (**1**), $Cp_2Y(THF)(H)_4Re(PMe_2Ph)_3$ (**2**), $Cp_2Y(THF)Re_2H_7(PMe_2Ph)_4$ (**3**), and $Cp_2LuRe_2H_7(PMe_2Ph)_4$ (**4**)

	1	2	3	4
formula	$C_{50}H_{54}OP_2YRe \cdot C_7H_8$	$C_{38}H_{55}OP_3YRe$	$C_{42}H_{69}OP_4YRe_2$	$C_{42}H_{61}P_4LuRe_2$
fw	1100.1	895.8	1223.2	1237.2
cryst system	monoclinic	orthorhombic	monoclinic	monoclinic
space group	$P2_1/c$ (C_{2h}^5; No. 14)	$Pca2_1$ (C_{2v}^5; No. 29)	$P2_1/n$	$P2_1/c$ (C_{2h}^5; No. 14)
a, Å	19.886 (4)	21.537 (4)	11.9546 (16)	17.677 (4)
b, Å	9.8014 (15)	11.734 (2)	31.613 (4)	12.960 (2)
c, Å	25.815 (5)	30.142 (4)	12.571 (2)	19.199 (3)
β, deg	102.653 (15)		92.376 (11)	90.990 (16)
V, Å^3	4909.5 (15)	7617 (2)	4746.5 (11)	4397.7 (14)
Z	4	8	4	4
D_{calcd}, Mg/m^3	1.488	1.562	1.712	1.87
radiation (λ = 0.710 730 Å)	Mo Kα	Mo Kα	Mo Kα	Mo Kα
T, K	183	193	213	183
μ(Mo Kα), mm^{-1}	3.78	4.90	6.54	7.97
R_F; R_{wF}[a]	5.0%; 4.7%	5.8%; 7.1%	6.1%; 9.0%	4.9%; 5.8%

[a] $R_F = 100[\sum||F_o| - |F_c||/\sum|F_o|]$; $R_{wF} = 100[\sum w(|F_o| - |F_c|)^2/\sum w|F_o|^2]$.

methods. Carbon monoxide (Air Products), ethylene (Matheson), propylene (Matheson), diphenylacetylene (Aldrich), and triphenylphosphine (Aldrich) were used as obtained. Styrene (Aldrich) was dried over 4-Å molecular sieves and vacuum transferred prior to use. Carbon dioxide (Matheson) was dried over P_2O_5 prior to use. Initial syntheses of the mixed-metal complexes were done by adding a cold solution of the metal alkyl to a cold solution of the metal hydride and allowing the system to slowly warm to room temperature. Later, it was found that the same results could be obtained by mixing the two powders and adding solvent.

$Cp_2Ln(THF)H_6Re(PPh_3)_2$. $ReH_7(PPh_3)_2$ (0.200 g, 0.280 mmol) was added to a flask containing $Cp_2YMe(THF)$ (0.086 g, 0.280 mmol) in 10 mL of THF. After the resulting solution was stirred for 0.5 h, THF solvent was removed in vacuo to yield $Cp_2Y(THF)H_6Re(PPh_3)_2$, **1** (0.260 g, 0.258 mmol, 93%). ^{1}H NMR (C_6D_6, 25 °C): −5.65 (t of d, J_{H-P} = 13.4 Hz, J_{H-Y} = 8.3 Hz, Re–H), 1.25 (s, THF), 3.42 (s, THF), 6.15 (s, Cp), 6.96 (m, Ph), 7.74 (t, J = 7.2 Hz, Ph). $\{^1H\}^{31}P$ (C_6D_6, 25 °C): 36.9 (d, J_{P-Y} = 4.4 Hz). IR (Nujol): 1958 w, 1898 w, 1767 w, 1479 m, 1433 s, 1089 m cm^{-1}. Anal. Calcd for $C_{50}H_{54}OP_2YRe$: Y, 8.8. Found: Y, 8.4.

$Cp_2Lu(THF)H_6Re(PPh_3)_2$ can be prepared similarly in 91% yield. ^{1}H NMR (C_6D_6, 25 °C): −5.30 (t, J_{H-P} = 13.8 Hz, Re–H), 1.22 (s, THF), 3.42 (s, THF), 6.11 (s, Cp), 6.95 (m, Ph), 7.73 (t, J = 7.2 Hz, Ph). $\{^1H\}^{31}P$ (C_6D_6, 25 °C): 37.7 (s). IR (Nujol): 1949 w, 1894 m, 1818 w, 1778 w, 1479 m, 1433 s, 1091 m cm^{-1}. Anal. Calcd for $C_{50}H_{54}OP_2LuRe$: Lu, 16.0. Found: Lu, 16.5.

X-ray Data Collection, Structure Determination, and Refinement for $Cp_2Y(THF)H_6Re(PPh_3)_2$, 1. A pale yellow crystal of approximate dimensions 0.13 × 0.27 × 0.30 mm grown from a concentrated 3:1 toluene/THF solution over the course of 90 h at −35 °C was immersed in Paraton-N (lube oil additive), mounted on a glass fiber, and transferred to the Syntex $P2_1$ diffractometer which is equipped with a modified LT-1 apparatus. Subsequent setup operations (determination of accurate unit cell dimensions and orientation matrix) and collection of low-temperature (183 K) intensity data were carried out using standard techniques similar to those of Churchill.[10] Details appear in Table I.

All 6633 data were corrected for the effects of absorption and for Lorentz and polarization effects and placed on an approximately absolute scale by means of a Wilson plot. A careful examination of a preliminary data set revealed the systematic extinctions $0k0$ for $k = 2n + 1$ and $h0l$ for $l = 2n + 1$; the diffraction symmetry was $2/m$. The centrosymmetric monoclinic space group $P2_1/c$ (C_{2h}^5; No. 14) is thus uniquely defined.

All crystallographic calculations were carried out using either our locally modified version of the UCLA Crystallographic Computing Package[11] or the SHELXTL PLUS program set.[12] The analytical scattering factors for neutral atoms were used throughout the analysis;[13a] both the real ($\Delta f'$) and imaginary ($i\Delta f''$) components of anomalous dispersion[13b] were included. The quantity minimized during least-squares analysis was $\sum w(|F_o| - |F_c|)^2$, where $w^{-1} = \sigma(|F_o|) + 0.0006|F_o|)^2$.

The structure was solved by direct methods (SHELXTL PLUS) and refined by full-matrix least-squares techniques. Hydrogen atom contributions were included using a riding model with d(C–H) = 0.96 Å and U(iso) = 0.08 Å^2. The positions of all six hydride ligands were determined from a series of difference-Fourier maps. The temperature factor of H(1) could not be refined and was fixed at 0.05 Å^2. A toluene solvent of crystallization was located and refined anisotropically. At convergence, R_F = 5.0%, R_{wF} = 4.7%, and GOF = 1.14 for 582 variables refined against those 5022 data with $|F_o| > 3.0\sigma(|F_o|)$. A final difference-Fourier map was devoid of significant features, with ρ(max) = 0.74 e Å^{-3} at a distance of 1.58 Å from C(62).

$Cp_2Ln(THF)H_4Re(PMe_2Ph)_3$. $ReH_5(PMe_2Ph)_3$ (0.150 g, 0.248 mmol) was added to a flask containing $Cp_2YMe(THF)$ (0.090 g, 0.293 mmol) in 10 mL of toluene. After the resulting solution was stirred for 1.5 h at 70 °C, the solvent was removed in vacuo to yield an oily yellow-orange solid. The solid was triturated with 10 mL of hexane to give a powder. The precipitate was isolated by filtration through a fine-porosity frit to remove the excess hexane-soluble $Cp_2YMe(THF)$. $Cp_2Y(THF)H_4Re(PMe_2Ph)_3$, **2**, was obtained as a yellow powder (0.118 g, 0.132 mmol, 53%). ^{1}H NMR (C_6D_6, 25 °C): −7.90 (m, Re–H), 1.24 (s, THF), 1.80 (d, J_{P-H} = 7.2 Hz, Me), 3.45 (s, THF), 6.20 (s, Cp), 7.07 (t, J = 6.5 Hz, Ph), 7.19 (t, J = 6.8 Hz, Ph), 7.76 (t, J = 8.6 Hz). $\{^{31}P\}^1$H NMR (C_6D_6, 25 °C): −7.90 (d, J_{Y-H} = 14.7 Hz, Re–H). $\{^1H\}^{31}P$ (C_6D_6, 25 °C): −14.13 (d, J_{P-Y} = 7.0 Hz). IR (Nujol): 2714 m, 1896 m, 1651 w, 1435 m, 1012 m cm^{-1}. Anal. Calcd for $C_{38}H_{55}OP_3YRe$: Y, 9.9. Found: Y, 10.2.

$Cp_2Lu(THF)H_4Re(PMe_2Ph)_3$ can be prepared by the same procedure in 56% yield. ^{1}H NMR (C_6D_6, 25 °C): −7.36 (q, J_{H-P} = 16.0 Hz, Re–H), 1.13 (s, THF), 1.76 (d, J_{H-P} = 7.2 Hz, Me), 3.42 (s, THF), 6.16 (s, Cp), 7.08 (t, J = 7.6 Hz, Ph), 7.19 (t, J = 6.8 Hz, Ph), 7.81 (t, J = 6.5 Hz, Ph). $\{^1H\}^{31}P$ (C_6D_6, 25 °C): −13.70 (s). IR (Nujol): 2723 w, 1902 w, 1653 w, 1437 m, 1012 s cm^{-1}. Anal. Calcd for $C_{38}H_{55}OP_3LuRe$: Lu, 17.8. Found: Lu, 18.2.

$Cp_2Y(THF)H_4Re(PPh_3)_3$. A 0.5-mL toluene-d_8 solution of $Cp_2YMe(THF)$ (0.005 g, 0.015 mmol) was added to an NMR tube containing $ReH_5(PPh_3)_3$ (0.015 g, 0.015 mmol). The sample was heated to 85 °C for 2.5 h. Over this period, 50% conversion (by ^{1}H NMR) to $Cp_2Y(THF)H_4Re(PPh_3)_3$ occurred. The remainder of the unreacted $ReH_5(PPh_3)_3$ was observed. Prolonged heating or higher temperatures leads to decomposition. ^{1}H NMR (C_6D_6, 25 °C): −6.91 (br s, Re–H), 1.33 (s, THF), 3.50 (s, THF), 5.97 (s, Cp), 6.97 (m, Ph), 7.40 (br s, Ph). $\{^1H\}^{31}P$ (C_6D_6, 25 °C): 37.14 (s).

X-ray Data Collection, Structure Determination, and Refinement for $Cp_2Y(THF)H_4Re(PMe_2Ph)_3$, 2. A light yellow crystal of approximate dimensions 0.17 × 0.30 × 0.33 mm was grown from a concentrated hexane solution at −35 °C over the course of 4 weeks and was handled as described above for **1**. Details appear in Table I.

All 7408 data were corrected for the effects of absorption and for Lorentz and polarization effects and placed on an approximately absolute scale. A careful examination of a preliminary data set revealed the systematic extinctions $0kl$ for $l = 2n + 1$ and $h0l$ for $h = 2n + 1$. The two possible orthorhombic space groups are the noncentrosymmetric $Pca2_1$

(9) Evans, W. J.; Meadows, J. H.; Hunter, W. E.; Atwood, J. L. *J. Am. Chem. Soc.* **1984**, *106*, 1291–1300.
(10) Churchill, M. R.; Lashewycz, R. A.; Rotella, F. J. *Inorg. Chem.* **1977**, *16*, 265–271.
(11) UCLA Crystallographic Computing Package, University of California, Los Angeles, CA, 1981. Strause, C. Personal communication.
(12) Nicolet Instrument Corp., Madison, WI, 1988.
(13) *International Tables for X-ray Crystallography*; Kynoch Press: Birmingham, England, 1974: (a) pp 99–101; (b) pp 149–150.

(C_{2v}^5; No. 29) or the centrosymmetric *Pbcm* (C_{2h}^{11}; No. 57) (standard setting of *Pcam*). All crystallographic calculations were carried out as described above for **1**.

Several methods (MITHRIL, SHELXTL, DIRDIF, Patterson) to solve the structure in the centrosymmetric space group were attempted, but none yielded a correct solution. The noncentrosymmetric space group was then tried (SHELXTL PLUS), and the positions of the rhenium, yttrium, and phosphorus atoms for two independent molecules were readily determined from a single "*E*-map". All non-hydrogen/hydride atoms were subsequently located from a series of difference-Fourier syntheses. When refinement was complete, it was noted that the fractional coordinates of atom pairs (e.g., Re(1), Re(2); Y(1), Y(2); P(1), P(5); etc.) appeared to be related to one another. This implies that the two molecules may be related by an inversion center, in which case the correct space group would be *Pbcm* and the correct model would be an "average" of the two independent molecules reported here. Attempts to resolve this problem have been unsuccessful. However, the derived results, interatomic distances, angles, etc. for the two independent molecules show no inconsistencies. While the ambiguity in the space group assignment is troublesome, the structure is otherwise correct and complete.

Full-matrix least-squares refinement of positional and thermal parameters (isotropic for carbon and oxygen atoms) led to convergence with $R_F = 5.8\%$, $R_{wF} = 7.1\%$, and GOF = 1.43 for 403 variables refined against those 5087 data with $|F_o| > 4.0\sigma(|F_o|)$. Hydrogen atom contributions were included using a riding model with d(C–H) = 0.96 Å and U(iso) = 0.08 Å^2. The positions of the hydride ligands could not be determined from the study and were therefore not included.

$Cp_2Y(THF)Re_2H_7(PMe_2Ph)_4$, 3. $Re_2H_8(PMe_2Ph)_4$ (0.300 g, 0.322 mmol) was added to a flask containing a THF solution of $Cp_2YMe(THF)$ (0.120 g, 0.392 mmol). After the resulting solution was stirred for 3.5 h, the solvent was removed in vacuo to leave a dark brown solid. The solid was washed with 2 × 5 mL of hexane to remove excess $Cp_2YMe(THF)$. $Cp_2Y(THF)Re_2H_7(PMe_2Ph)_4$ was isolated as a dark brown solid (0.279 g, 0.229 mmol, 71%). ^{1}H NMR (25 °C, C_6D_6): 7.55 (br s, Ph), 7.12 (t, J = 7 Hz, Ph), 7.03 (t, J = 7 Hz, Ph), 1.73 (pseudo doublet, J = 6.6 Hz, Me), –8.87 (br s, Re–H), 6.49 (s, Cp), 3.48 (s, THF), and 1.72 (s, THF). $\{^{31}P\}^1$H NMR (65 °C, toluene-d_8): –8.88 (d, J_{Y-H} = 7.2 Hz). $\{^{31}P\}^1$H NMR (80 °C, toluene-d_8): –8.88 (s). $\{^1H\}^{31}$P NMR (25 °C, THF): –9.63. IR (Nujol): 1962 m, 1936 m, 1583 w, 1278 w, 1012 m, 939 m, 908 m cm^{-1}. Anal. Calcd for $C_{46}H_{69}OP_4YRe_2$: Y, 7.3. Found: Y, 7.0.

X-ray Data Collection, Structure Determination, and Refinement for $Cp_2Y(THF)Re_2H_7(PMe_2Ph)_4$, 3. A bright red crystal of approximate dimensions 0.17 × 0.47 × 0.50 mm was grown from concentrated hexane at –35 °C over 72 h and was handled as described above for **1**. Details appear in Table I.

All 8771 data were corrected for the effects of absorption and for Lorentz and polarization effects and placed on an approximately absolute scale by means of a Wilson plot. A careful examination of a preliminary data set revealed the systematic extinctions $0k0$ for $k = 2n + 1$ and $h0l$ for $h + l = 2n + 1$; the diffraction symmetry was $2/m$. The centrosymmetric monoclinic space group $P2_1/n$, a nonstandard setting of $P2_1/c$ (C_{2h}^5; No. 14), is thus uniquely defined. Crystallographic calculations were carried out as described above for **1**. The quantity minimized during least-squares analysis was $\sum w(|F_o| - |F_c|)^2$, where $w^{-1} = \sigma^2(|F_o|) + 0.001(|F_o|)^2$.

The structure was solved by direct methods (SHELXTL PLUS) and refined by full-matrix least-squares techniques. Hydrogen atom contributions were included using a riding model with d(C–H) = 0.96 Å and U(iso) = 0.08 Å^2. The positions of the hydride ligands could not be determined from the study and were therefore not included. Refinement of positional and anisotropic thermal parameters (isotropic for C(11), C(44), C(73)) led to convergence with $R_F = 6.1\%$, $R_{wF} = 9.0\%$, and GOF = 2.16 for 473 variables refined against those 6616 data with $|F_o| > 4.0\sigma(|F_o|)$. A final difference-Fourier map was devoid of significant features, with ρ(max) = 2.5 e Å^{-3} at a distance of 0.99 Å from Re(1).

$Cp_2LuRe_2H_7(PMe_2Ph)_4$, 4. $Re_2H_8(PMe_2Ph)_4$ (0.300 g, 0.322 mmol) was added to a THF solution of $Cp_2LuMe(THF)$ (0.151 g, 0.386 mmol). After the resulting solution was stirred 3.5 h, the solvent was removed in vacuo to leave a dark brown solid. The solid was washed with 2 × 5 mL of hexane to remove excess $Cp_2LuMe(THF)$. $Cp_2LuRe_2H_7(PMe_2Ph)_4$ was isolated as a dark brown solid (0.272 g, 0.220 mmol, 68%). Alternatively, $Cp_2LuRe_2H_7(PMe_2Ph)_4$ may be synthesized from $[Cp_2LuMe]_2$ and $Re_2H_8(PMe_2Ph)_4$ in toluene solvent over 2.5 h. ^{1}H NMR (25 °C, C_6D_6): 7.54 (br s, Ph), 7.10 (m, Ph), 1.72 (pseudo doublet, J = 5.4 Hz, Me), –8.62 (br s, Re–H), 6.48 (s, Cp). $\{^1H\}^{31}$P NMR (25 °C, C_6D_6): –8.77 (s). IR (Nujol): 2924 s, 1966 w, 1936 m, 1433 m, 1261 w, 1095 m, 1012 m, 939 w, 906 m cm^{-1}. Anal. Calcd for $C_{42}H_{61}P_4LuRe_2$: Lu, 14.2. Found: Lu, 15.1.

X-ray Data Collection, Structure Determination, and Refinement for $Cp_2LuH_7Re_2(PMe_2Ph)_4$, 4. A dark brown crystal of approximate dimensions 0.15 × 0.17 × 0.18 mm was grown from hexane solutions at –35 °C over 48 h and was handled as described above for **1**. Details appear in Table I.

All 5995 data were corrected for the effects of absorption and for Lorentz and polarization effects and placed on an approximately absolute scale by means of a Wilson plot. A careful examination of a preliminary data set revealed the systematic extinctions $0k0$ for $k = 2n + 1$ and $h0l$ for $l = 2n + 1$; the diffraction symmetry was $2/m$. The centrosymmetric monoclinic space group $P2_1/c$ (C_{2h}^5; No. 14) is, thus, uniquely defined.

Crystallographic calculations were carried out as described above for **1**. The quantity minimized during least-squares analysis was $\sum w(|F_o| - |F_d|)^2$, where $w^{-1} = \sigma^2(|F_o|) + 0.0004(|F_o|)^2$. The structure was solved by direct methods (SHELXTL PLUS) and refined by full-matrix least-squares techniques. Hydrogen atom contributions were included using a riding model with d(C–H) = 0.96 Å and U(iso) = 0.08 Å^2. The positions of the hydride ligands could not be determined from the study and were therefore not included. Refinement of positional and thermal parameters (isotropic for all carbon atoms) led to convergence with $R_F = 4.9\%$, $R_{wF} = 5.8\%$, and GOF = 1.62 for 232 variables refined against those 4253 data with $|F_o| > 4.0\sigma(|F_o|)$. A final difference-Fourier map was featureless, with ρ(max) = 1.61 e Å^{-3} at a distance of 0.80 Å from C(15).

$Cp_2YRe_2H_7(PMe_2Ph)_4$. $Cp_2Y(THF)Re_2H_7(PMe_2Ph)_4$ was dissolved in an excess of toluene. This solvent was then removed in vacuo to yield $Cp_2YRe_2H_7(PMe_2Ph)_4$ as a greenish-brown powder. By the absence of THF, the ^{1}H NMR of $Cp_2YRe_2H_7(PMe_2Ph)_4$ shows this conversion to be quantitative. Alternatively, $Cp_2YRe_2H_7(PMe_2Ph)_4$ may be synthesized from $[Cp_2YMe]_2$ and $Re_2H_8(PMe_2Ph)_4$ in toluene solvent over 2.5 h. ^{1}H NMR (25 °C, C_6D_6): 7.60 (br s, Ph), 7.11 (m, Ph), 1.73 (pseudo doublet, J = 4.7 Hz, P–Me), –8.88 (br s, Re–H), 6.49 (s, Cp). $\{^1H\}^{31}$P NMR (25 °C, C_6D_6): –9.04 (Re–P). IR (Nujol): 2924 s, 1964 w, 1936 m, 1904 m, 1643 w, 1435 s, 1288 m, 1265 m, 1095 m, 933 m, 900 s cm^{-1}. Anal. Calcd for $C_{42}H_{61}P_4YRe_2$: Y, 7.7. Found: Y, 7.9.

Reaction of $Cp_2Y(THF)H_6Re(PPh_3)_2$ and Ethylene. Ethylene (2 atm, 19.6 mmol) was condensed into a flask containing a frozen (–196 °C) THF solution of $Cp_2Y(THF)H_6Re(PPh_3)_2$ (0.050 g, 0.049 mmol). The solution was then allowed to thaw to 25 °C and stirred for 12 h. THF solvent was then removed in vacuo to leave an oily dark residue. Reactions in toluene were done by the same procedure. ^{1}H NMR (C_6D_6, 25 °C): –9.95 (t, J = 40 Hz, Re–H), 4.26 (s, Cp for $CpReH_2(PPh_3)_2$), –5.03 (quintet, J = 10 Hz, Re–H for $Re_2H_8(PPh_3)_4$), –4.49 (quartet, J = 23 Hz, Re–H for $ReH_4(PPh_3)_3$), 1.30 (large singlet), and 0.85 (small broad singlet, polyethylene). $\{^1H\}^{31}$P NMR: 42.0 (s, P for $CpReH_2(PPh_3)_2$), 34.6 (s, Re–P for $ReH_4(PPh_3)_3$). After the NMR sample was taken, the reaction mixture was hydrolyzed by addition of 0.2 mL of H_2O under inert conditions. After the resulting mixture was stirred at 25 °C for 0.1 h, the solution was then opened to air and filtered through a 2-in. silica column to remove the metal-containing products. The volatiles were removed from the filtered solution to leave the oligomeric products, which were identified by mass spectrometry and ^{1}H NMR spectroscopy. MS (EI, 70 eV): m/z = 198, M$^+$, with a progression of peaks differing by 28.

Reaction of $Cp_2Y(THF)H_6Re(PPh_3)_2$ and Propylene. Propylene (2 atm, 19.6 mmol) was condensed into a flask containing a frozen (–196 °C) THF solution of $Cp_2Y(THF)H_6Re(PPh_3)_2$ (0.050 g, 0.049 mmol). The solution was then allowed to thaw to 25 °C and stirred for 12 h. THF solvent was then removed in vacuo to leave an oily dark residue. Reactions in toluene were done by the same procedure. ^{1}H NMR (C_6D_6, 25 °C): –9.95 (t, J = 40 Hz, Re–H), 4.26 (s, Cp for $CpReH_2(PPh_3)_2$), –5.03 (quintet, J = 10 Hz, Re–H for $Re_2H_8(PPh_3)_4$), –4.49 (quartet, J = 23 Hz, Re–H for $ReH_4(PPh_3)_3$), 1.2–1.5 (br m), and 0.85 (br m, polypropylene). $\{^1H\}^{31}$P NMR: 42.0 (s, P for $CpReH_2(PPh_3)_2$), 34.6 (s, P for $ReH_4(PPh_3)_3$). The sample was hydrolyzed as described above. MS (EI, 70 eV): m/z = 128, M$^+$.

Reaction of $Cp_2Y(THF)H_6Re(PPh_3)_2$ and Styrene. Styrene (2.040 g, 19.6 mmol) was added by syringe to a flask containing a THF solution (25 °C) of $Cp_2Y(THF)H_6Re(PPh_3)_2$ (0.050 g, 0.049 mmol). The solution was then stirred for 12 h. THF solvent was then removed in vacuo to leave an oily dark residue. Reactions in toluene were done by the same procedure. ^{1}H NMR (C_6D_6, 25 °C): –9.95 (t, J = 40 Hz, Re–H), 4.26 (s, Cp for $CpReH_2(PPh_3)_2$), –5.03 (quintet, J = 10 Hz, Re–H for $Re_2H_8(PPh_3)_4$), –4.49 (quartet, J = 23 Hz, Re–H for $ReH_4(PPh_3)_3$),

7.0–7.5 (br s), 5.8–6.5 (br s), and 1.2–1.7 (br m, polystyrene). $\{^1H\}^{31}P$ NMR: 42.0 (s, P for $CpReH_2(PPh_3)_2$), 34.6 (s, P for $ReH_4(PPh_3)_3$).

Reaction of 1 with PPh_3 and THF. PPh_3 (0.004 g, 0.0149 mmol) was added to $Cp_2Y(THF)H_6Re(PPh_3)_2$ (0.0150 g, 0.0149 mmol) (25 °C) in 0.5 mL of THF-d_8. After 0.3 h, ^1H NMR showed only unreacted **1** and free PPh_3. The mixture was heated at 70 °C for 2 h, after which unreacted $Cp_2Y(THF)H_6Re(PPh_3)_2$ and very minor amounts of decomposition product were observed. One equivalent of THF-d_8 was added at 25 °C to a (0.5 mL) C_6D_6 NMR sample containing **1** (0.015 g, 0.0149 mmol). The THF resonances in the ^1H NMR spectrum shift (3.42 to 3.52, 1.29 to 1.35 ppm) toward those of free THF (3.60, 1.40 ppm). Five equivalents of THF-d_8 cause a shift to 3.58 and 1.39 ppm; i.e., virtually all of the bound protio THF is replaced by THF-d_8.

Results and Discussion

In the selection of transition metals to couple with lanthanide metals, rhenium systems were chosen because of the availability of many rhenium polyhydrides representing several oxidation states.[14] Among the lanthanide metals, yttrium and lutetium were chosen because they form diamagnetic complexes and their small size make it easier to generate isolable sterically saturated complexes.[15]

$ReH_7(PPh_3)_2$ was chosen to react with $Cp_2LnMe(THF)$ because it readily loses a proton to hydride reagents[16] (e.g., KH), and could thus react in an analogous fashion with Ln–R bonds. Hydride complexes containing carbon monoxide ligands are fair Bronsted acids[17] but were avoided because of their ability to form isocarbonyl linkages, M–C–O–Ln.[18] Transition metal hydride complexes with phosphine ligands are less Bronsted acidic, but the polar character of the lanthanide alkyl bond was sufficient to give the desired elimination of methane.

Synthesis of $Cp_2Ln(THF)H_6Re(PPh_3)_2$. The reaction of $ReH_7(PPh_3)_2$ with $Cp_2LnMe(THF)$ proceeds rapidly in THF with CH_4 (identified by ^1H NMR) evolution observed on addition of solvent (eq 2). Removal of solvent in vacuo leaves $Cp_2Ln(THF)(H)_6Re(PPh_3)_2$ as a beige solid in nearly quantitative yield.

$$ReH_7(PPh_3)_2 + Cp_2LnMe(THF) \rightarrow Cp_2Ln(THF)(H)_6Re(PPh_3)_2 + CH_4 \quad (2)$$

$$Ln = Y, Lu$$

The ^1H NMR spectrum of $Cp_2Y(THF)(H)_6Re(PPh_3)_2$, **1**, exhibits resonances for bound THF and a hydride resonance consisting of a six-line doublet of triplet pattern at –5.65 ppm with J_{H-P} = 13.4 Hz and J_{H-Y} = 8.3 Hz. When the sample is cooled to –88 °C, the hydride resonance broadens into the baseline, but no new resonances were observed. Interestingly, at –60 °C, the two THF resonances broaden into the baseline, and on further cooling to –88 °C, four new resonances appear. The resolution of four resonances may arise because rapid rotation around the THF oxygen–yttrium bond has been slowed in this crowded environment.

The presence of only one hydride resonance at room temperature is consistent with rapid fluxionality of all six hydride ligands about the two metal centers. The yttrium to hydride coupling indicates that the molecule does not exist as solvent separated ion pairs in solution (benzene or THF) and implies the presence of bridging hydride ligands to yttrium. The smaller magnitude of the J_{H-Y} coupling constant compared to J_{H-Y} = 27.0 Hz in $[Cp_2Y(\mu\text{-}H)(THF)]_2$[19] may be attributed to the rapid fluxionality of the hydride ligands about rhenium and yttrium in bridging and terminal locations. Since the observed coupling constant is an average coupling of six hydride ligands, it can be used to predict the number of hydride ligands that are interacting with yttrium via rhenium to yttrium bridges. The fact that the observed average coupling constant is about one-third of a typical Y–(μ-H) coupling constant is consistent with two of the six hydride ligands bridging from rhenium to yttrium. This solution-phase conclusion is confirmed in the solid state by X-ray crystallography (see below), where four of the hydride ligands are found to be terminal on rhenium.

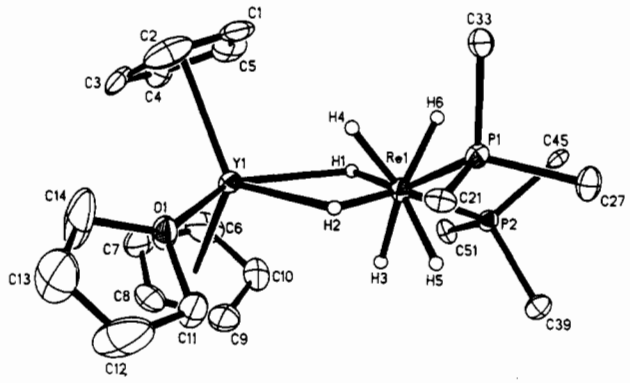

Figure 1. ORTEP diagram of $Cp_2Y(THF)(H)_6Re(PPh_3)_2$, **1**, in which phenyl ring carbons are omitted for clarity.

The $\{^1H\}^{31}P$ NMR spectrum is consistent with the ^1H NMR and shows a doublet with J_{P-Y} = 4.4 Hz. This phosphorus resonance remains unchanged down to –88 °C. For $Cp_2Lu(THF)(H)_6Re(PPh_3)_2$, the hydride resonance is a triplet with J_{H-P} = 13.8 Hz and the $\{^1H\}^{31}P$ resonance is a singlet.

When $Cp_2Y(THF)(H)_6Re(PPh_3)_2$ is dissolved in toluene, followed by removal of solvent in vacuo, THF is retained (^1H NMR). Even under a dynamic vacuum at 10^{-5} Torr, THF is not lost. **1** undergoes only 15% decomposition in benzene at 70 °C but forms $CpReH_2(PPh_3)_2$[20] and white insoluble materials in toluene at 110 °C within 3 h. Attempts to form $Cp_2Ln(H)_6Re(PPh_3)_2$ directly by reaction of $ReH_7(PPh_3)_2$ and $[Cp_2LnMe]_2$ in toluene solvent led to complex mixtures of products. **1** does not react with PPh_3 even at 70 °C, but exchange with free THF does occur at 25 °C.

Molecular Structure of $Cp_2Y(THF)(H)_6Re(PPh_3)_2$, 1. The X-ray crystallographic study revealed a bimetallic structure for **1** (Figure 1). Selected bond angles and distances for $Cp_2Y(THF)(H)_6Re(PPh_3)_2$ are given in Table II. All six hydride ligands were located in the structure determination, where H(1) and H(2) form Re–H–Y bridges and H(3), H(4), H(5), and H(6) were found to be terminally bound to rhenium. None of the hydrogen atoms are within covalent bonding distance of each other; the shortest nonbonding distances is 1.416 Å between H(2) and H(4). This shows the absence of an η^2-dihydrogen species in the solid state.[21] The coordination environment about yttrium is very similar to that reported for $[(MeC_5H_4)_2Y(\mu\text{-}H)(THF)]_2$. Hence, it is unnecessary to invoke any metal–metal bonding to explain the connectivity of the structure. It is interesting to note, however, that the 3.088 (1)-Å Re–Y distance lies within the sum of the metallic radii of these elements, 3.16 Å.[22] The Re–Y distance is only slightly longer than the unsupported 3.0277 (6)-Å

(14) Hlatky, G. G.; Crabtree, R. H. *Coord. Chem. Rev.* **1985**, *65*, 1–48.
(15) (a) Evans, W. J. In *The Chemistry of the Metal-Carbon Bond*; Hartley, F. R., Patai, S., Eds.; Wiley: New York, 1982; Chapter 12. (b) Evans, W. J. *Adv. Organomet. Chem.* **1985**, *24*, 131–177.
(16) Alvarez, D., Jr.; Lundquist, E. G.; Ziller, J. W.; Evans, W. J.; Caulton, K. G. *J. Am. Chem. Soc.* **1989**, *111*, 8392–8398.
(17) Edidin, R. T.; Sullivan, J. M.; Norton, J. R. *J. Am. Chem. Soc.* **1987**, *109*, 3745–3953 and references therein.
(18) Boncella, J. M.; Andersen, R. A. *Inorg. Chem.* **1984**, *23*, 432–437 and references therein.
(19) Evans, W. J.; Meadows, J. H.; Wayda, A. L.; Hunter, W. E.; Atwood, J. L. *J. Am. Chem. Soc.* **1982**, *104*, 2008–2014.
(20) Jones, W. D.; Maguire, J. A. *Organometallics* **1987**, 1301–1311.
(21) Crabtree, R. H.; Hamilton, D. G. *Adv. Organomet. Chem.* **1988**, *28*, 299–338.
(22) Wells, A. F. *Structural Inorganic Chemistry*, 4th ed.; Clarendon Press: Oxford, England, 1975; p 1022.

Table II. Selected Bond Distances (Å) and Angles (deg) for $Cp_2Y(THF)(H)_6Re(PPh_3)_2$, **1**[a]

Interatomic Distances (Å) with Esd's			
Re(1)–Y(1)	3.088 (1)	Re(1)–P(1)	2.376 (2)
Re(1)–P(2)	2.396 (3)	Re(1)–H(1)	1.588 (84)
Re(1)–H(2)	1.479 (75)	Re(1)–H(3)	1.519 (110)
Re(1)–H(4)	1.501 (80)	Re(1)–H(5)	1.569 (78)
Re(1)–H(6)	1.528 (94)	Y(1)–O(1)	2.369 (7)
Y(1)–H(1)	2.282 (87)	Y(1)–H(2)	2.437 (61)
Y(1)–C(1)	2.709 (13)	Y(1)–C(2)	2.678 (12)
Y(1)–C(3)	2.663 (10)	Y(1)–C(4)	2.668 (10)
Y(1)–C(5)	2.664 (11)	Y(1)–C(6)	2.636 (9)
Y(1)–C(7)	2.687 (11)	Y(1)–C(8)	2.698 (12)
Y(1)–C(9)	2.683 (12)	Y(1)–C(10)	2.669 (11)
Y(1)–Cent(1)	2.398	Y(1)–Cent(2)	2.396
Interatomic Angles (deg) with Esd's			
Y(1)–Re(1)–P(1)	129.3 (1)	Y(1)–Re(1)–P(2)	124.2 (1)
P(1)–Re(1)–P(2)	106.4 (1)	Y(1)–Re(1)–H(1)	45.7 (32)
P(1)–Re(1)–H(1)	153.5 (35)	P(2)–Re(1)–H(1)	83.1 (34)
Y(1)–Re(1)–H(2)	50.7 (24)	P(1)–Re(1)–H(2)	85.8 (26)
P(2)–Re(1)–H(2)	153.4 (30)	H(1)–Re(1)–H(2)	96.4 (41)
Y(1)–Re(1)–H(3)	74.3 (37)	P(1)–Re(1)–H(3)	134.8 (35)
P(2)–Re(1)–H(3)	68.3 (39)	H(1)–Re(1)–H(3)	71.7 (49)
H(2)–Re(1)–H(3)	86.2 (49)	Y(1)–Re(1)–H(4)	59.8 (26)
P(1)–Re(1)–H(4)	75.7 (26)	P(2)–Re(1)–H(4)	148.4 (30)
H(1)–Re(1)–H(4)	83.4 (44)	H(2)–Re(1)–H(4)	56.8 (42)
H(3)–Re(1)–H(4)	132.7 (48)	Y(1)–Re(1)–H(5)	119.3 (28)
P(1)–Re(1)–H(5)	66.4 (30)	P(2)–Re(1)–H(5)	83.3 (31)
H(1)–Re(1)–H(5)	140.0 (46)	H(2)–Re(1)–H(5)	80.2 (40)
H(3)–Re(1)–H(5)	68.4 (46)	H(4)–Re(1)–H(5)	124.0 (43)
Y(1)–Re(1)–H(6)	108.9 (30)	P(1)–Re(1)–H(6)	82.1 (31)
P(2)–Re(1)–H(6)	71.3 (36)	H(1)–Re(1)–H(6)	77.6 (44)
H(2)–Re(1)–H(6)	134.7 (46)	H(3)–Re(1)–H(6)	131.3 (52)
H(4)–Re(1)–H(6)	78.0 (47)	H(5)–Re(1)–H(6)	131.8 (40)
Re(1)–Y(1)–O(1)	101.0 (1)	Re(1)–Y(1)–H(1)	29.9 (22)
O(1)–Y(1)–H(1)	130.6 (21)	Re(1)–Y(1)–H(2)	28.0 (18)
O(1)–Y(1)–H(2)	73.0 (18)	H(1)–Y(1)–H(2)	57.9 (28)
Cent(1)–Y(1)–Re(1)	112.4	Cent(2)–Y(1)–Re(1)	113.9
Cent(1)–Y(1)–O(1)	102.2	Cent(2)–Y(1)–O(2)	99.9
Cent(1)–Y(1)–H(1)	103.8	Cent(2)–Y(1)–H(1)	100.1
Cent(1)–Y(1)–H(2)	116.2	Cent(2)–Y(1)–H(2)	120.4
Cent(1)–Y(1)–Cent(2)	123.0		
Y(1)–O(1)–C(11)	120.6 (6)	Y(1)–O(1)–C(14)	128.8 (6)
C(11)–O(1)–C(14)	107.6 (8)	Re(1)–H(1)–Y(1)	104.4 (45)
Re(1)–H(2)–Y(1)	101.2 (33)		

[a] Cent(1) is the centroid of the C(1)–C(5) ring. Cent(2) is the centroid of the C(6)–C(10) ring.

Th–Ru bond in $(C_5Me_5)_2Th(I)Ru(CO)_2(C_5H_5)$[23] (9-coordinate Y^{3+} is 0.025 Å larger than 8-coordinate Th^{4+} according to Shannon).[24]

An interesting structural feature in **1** is the retention of a THF ligand on yttrium (Y–O = 2.369 (7) Å), in spite of a fair amount of steric crowding in the molecule (see below). The Y–O distance is shorter than the 2.460 (8)-Å distance found $[(MeC_5H_4)_2Y(\mu\text{-}H)(THF)]_2$.[18] Steric crowding is quite evident in the small (Cp centroid)–Y–(Cp centroid) angle of 123.0°. This angle is smaller that any previously reported for Cp_2Y systems (cf. 125.5° in $Cp_2Y(CH_2SiMe_3)_2^-$).[25]

The ReH_6P_2 moiety in **1** may be described as having a distorted dodecahedral geometry about rhenium defined by two approximately perpendicular trapezoidal planes (H(3), H(5), P(1), H(1)) and (H(6), H(4), H(2), P(2)), each containing rhenium (Figure 2a). This geometry is reasonable in that it places the large phosphorus atoms in the larger, less hindered positions of the trapezoids. A similar geometry was found for the ReH_6P_2 moiety in $[K(THF)_2ReH_6(PPh_3)_2]_2$.[16] A comparison of the two ReH_6P_2 fragments using atomic coordinates (see supplementary material) showed a good match for the ReP_2 moieties, which contain the most accurately located nuclei. The largest deviations between the two molecules occur in the hydrogen pairs (H(1), H(4)), (H(3), H(1)), and (H(4), H(3)), which may occur because a bridging hydride ligand from one molecule is being compared to a terminal hydride ligand in the other molecule. In spite of this, the geometric similarities between the two ReH_6P_2 fragments are quite evident when they are superimposed (Figure 2b) and the molecules are virtually the same within the errors of each structure determination.

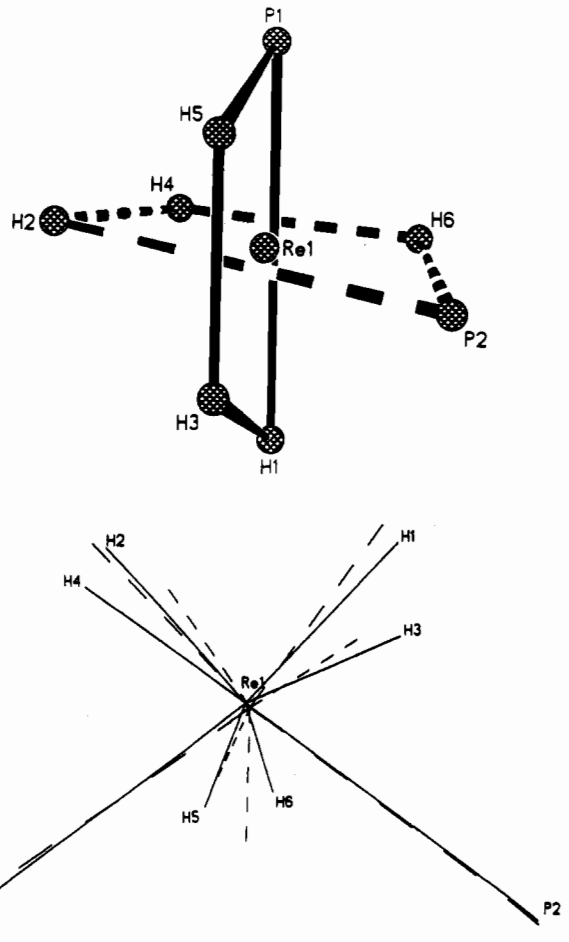

Figure 2. (a) Top: Idealized orthogonal trapezoidal units of the dodecahedral coordination geometry about rhenium in $Cp_2Y(THF)(H)_6Re(PPh_3)_2$, **1**. (b) Bottom: Model fit of the ReH_6P_2 moieties in $Cp_2Y(THF)(H)_6Re(PPh_3)_2$, **1** (solid lines), and $[K(THF)_2ReH_6(PPh_3)_2]_2$ (dashed lines).

Viewing the molecule down the Re–Y axis (Figure 3), it is noteworthy that the molecule adopts a somewhat twisted conformation, but the Y(1), Re(1), P(1), and P(2) atoms are nearly (within ca. 0.2 Å) planar. This is not unlike the geometry found for the related zirconium–rhenium complex $Cp_2Zr(Cl)(H)_6Re(PPh_3)_2$.[26] The twisting may be attributed to an unfavorable steric interaction between the THF ligand and the large PPh_3 ligands. Consistent with this, the P(1)–Re–P(2) angle in **1**, 106.4 (1)°, is much smaller than that in nine-coordinate $ReH_7(PPh_3)_2$, 138.9°.[27]

Reactions of $ReH_5(PR_3)_3$ and $Cp_2LnMe(THF)$. The rapid reaction between $ReH_7(PPh_3)_2$ and $Cp_2LnMe(THF)$ to form $Cp_2Ln(THF)(H)_6Re(PPh_3)_2$ suggested that $Cp_2LnMe(THF)$ could react with less Bronsted acidic polyhydride complexes such as $ReH_5(PR_3)_3$. However, the large steric bulk that results from the presence of three phosphine ligands and the observed steric crowding in **1** meant that reaction might not occur or might lead to an ionic charge separated salt such as $Cp_2Ln(L)_z^+/MH_xP_3^-$.

(23) Sternal, R. S.; Brock, C. P.; Marks, T. J. *J. Am. Chem. Soc.* **1985**, *107*, 8270–8272.
(24) Shannon, R. D. *Acta Crystallogr.* **1976**, *A32*, 751–767.
(25) Evans, W. J.; Dominguez, R.; Levan, K. R.; Doedens, R. J. *Organometallics* **1985**, *4*, 1836–1841.
(26) Sartain, W. J.; Lundquist, E. G.; Huffman, J. C.; Streib, W. E.; Caulton, K. G. *J. Mol. Catal.* **1989**, *56*, 20–35.
(27) Howard, J. A. K.; Johnson, O.; Koetzle, T. F.; Spencer, J. L. *Inorg. Chem.* **1987**, *26*, 2930.

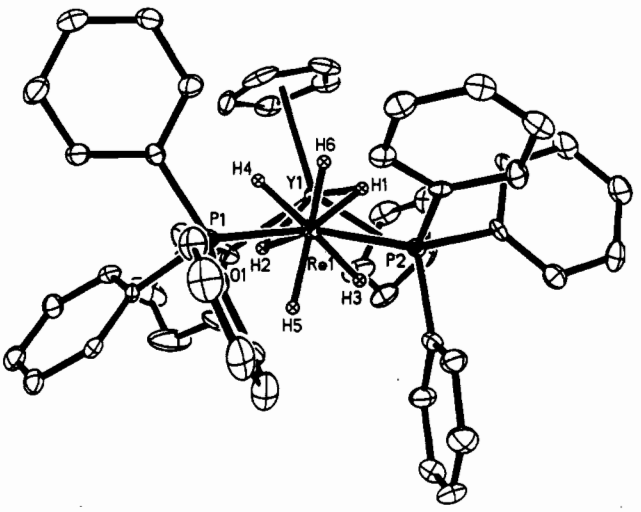

Figure 3. ORTEP view of $Cp_2Y(THF)(H)_6Re(PPh_3)_2$, **1**, looking down the Re–Y axis. Carbon atom labels have been omitted for clarity.

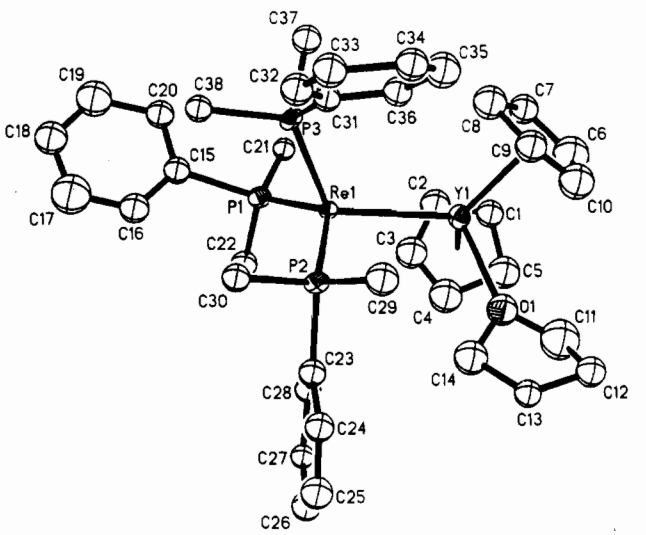

Figure 4. ORTEP diagram of one of the independent molecules found in the unit cell of $Cp_2Y(THF)(H)_4Re(PMe_2Ph)_3$, **2**.

Consistent with this, reaction of $ReH_5(PMe_2Ph)_3$ and $Cp_2LnMe(THF)$ (Ln = Y, Lu) in toluene or THF solvent occurs more slowly than the formation of **1**. However, methane elimination again proved to be a successful synthetic route and after 3 h at room temperature gave $Cp_2Ln(THF)(H)_4Re(PMe_2Ph)_3$ and CH_4 gas (identified by ^1H NMR) (eq 3). Under these conditions, some starting materials remain. When the reaction mixture is heated to 70 °C in toluene solvent, complete conversion to $Cp_2Ln(THF)(H)_4Re(PMe_2Ph)_3$ occurs after 1.5 h.

$$ReH_5(PMe_2Ph)_3 + Cp_2LnMe(THF) \rightarrow Cp_2Ln(THF)(H)_4Re(PMe_2Ph)_3 + CH_4 \quad (3)$$

The ^1H NMR spectra of these $Cp_2Ln(THF)(H)_4Re(PMe_2Ph)_3$ complexes show only one resonance for the hydride ligands at 25 °C. This is indicative of a fluxional process involving the four hydride ligands. For $Cp_2Y(THF)(H)_4Re(PMe_2Ph)_3$, the hydride resonance (C_6D_6, 25 °C) is a complicated multiplet centered at −7.90 ppm. When a toluene-d_8 sample is cooled to −88 °C, this resonance broadens, but the coalescence temperature was not reached before the solvent froze. When the phosphorus nuclei are decoupled in the ^1H NMR (C_6D_6, 25 °C), the hydride resonance becomes a doublet, J_{H-Y} = 14.7 Hz. It is evident that the complicated ^1H NMR spectrum arises from the similarity in the magnitudes of the two coupling constants since, for $Cp_2Lu(THF)(H)_4Re(PMe_2Ph)_3$, J_{P-H} = 16.0 Hz.

Table III. Selected Bond Distances (Å) and Angles (deg) for $Cp_2Y(THF)(H)_4Re(PMe_2Ph)_3$, **2**[a]

Interatomic Distances (Å) with Esd's			
Re(1)–Y(1)	3.111 (5)	Re(1)–P(1)	2.351 (7)
Re(1)–P(2)	2.351 (6)	Re(1)–P(3)	2.337 (7)
Y(1)–O(1)	2.386 (22)	Y(1)–C(1)	2.708 (31)
Y(1)–C(2)	2.709 (30)	Y(1)–C(3)	2.632 (31)
Y(1)–C(4)	2.677 (32)	Y(1)–C(5)	2.721 (34)
Y(1)–C(6)	2.760 (35)	Y(1)–C(7)	2.722 (29)
Y(1)–C(8)	2.684 (28)	Y(1)–C(9)	2.727 (30)
Y(1)–C(10)	2.789 (36)	Y(1)–Cnt(1)	2.430
Y(1)–Cnt(2)	2.453		
Re(2)–Y(2)	3.108 (5)	Re(2)–P(4)	2.340 (6)
Re(2)–P(5)	2.368 (7)	Re(2)–P(6)	2.337 (7)
Y(2)–O(2)	2.332 (19)	Y(2)–C(41)	2.679 (21)
Y(2)–C(42)	2.704 (30)	Y(2)–C(43)	2.783 (25)
Y(2)–C(44)	2.757 (29)	Y(2)–C(45)	2.693 (27)
Y(2)–C(46)	2.763 (33)	Y(2)–C(47)	2.699 (28)
Y(2)–C(48)	2.769 (27)	Y(2)–C(49)	2.765 (29)
Y(2)–C(50)	2.705 (29)	Y(2)–Cnt(3)	2.453
Y(2)–Cnt(4)	2.452		
Interatomic Angles (deg) with Esd's			
Y(1)–Re(1)–P(1)	105.8 (2)	Y(1)–Re(1)–P(2)	112.4 (2)
P(1)–Re(1)–P(2)	127.5 (3)	Y(1)–Re(1)–P(3)	123.4 (2)
P(1)–Re(1)–P(3)	96.1 (3)	P(2)–Re(1)–P(3)	91.7 (3)
Re(1)–Y(1)–O(1)	99.0 (5)	Re(1)–Y(1)–Cnt(1)	117.2
Re(1)–Y(1)–Cnt(2)	114.9	O(1)–Y(1)–Cnt(1)	101.5
O(1)–Y(1)–Cnt(2)	99.1	Cnt(1)–Y(1)–Cnt(2)	119.3
Y(2)–Re(2)–P(4)	111.6 (2)	Y(2)–Re(2)–P(5)	107.6 (2)
P(4)–Re(2)–P(5)	126.6 (3)	Y(2)–Re(2)–P(6)	123.0 (2)
P(4)–Re(2)–P(6)	92.5 (3)	P(5)–Re(2)–P(6)	95.3 (3)
Re(2)–Y(2)–O(2)	100.9 (5)	Re(2)–Y(2)–Cnt(3)	116.3
Re(2)–Y(2)–Cnt(4)	117.6	O(2)–Y(2)–Cnt(3)	101.0
O(2)–Y(2)–Cnt(4)	97.2	Cnt(3)–Y(2)–Cnt(4)	117.8

[a] Cnt(1) is the centroid of the C(1)–C(5) ring. Cnt(2) is the centroid of the C(6)–C(10) ring. Cnt(3) is the centroid of the C(41)–C(45) ring. Cnt(4) is the centroid of the C(46)–C(50) ring.

As described above for **1**, this observed coupling constant may be used to predict that there are two hydride ligands bridging from rhenium to yttrium and two terminal hydride ligands on rhenium. In this case, no direct comparison to the X-ray crystallographic study can be made because the four hydride ligands were not located in the structure determination (see below). However, the presence of two bridging hydrides gives a nine-coordinate yttrium center as is found for **1** and $[(MeC_5H_4)_2Y(\mu\text{-}H)(THF)]_2$.[18] Moreover, the presence of a considerable amount of steric congestion in the molecule (see below) may prevent the $ReH_4(PMe_2Ph)_3$ moiety from adopting the orientation necessary for placing a third hydride ligand in a bridging location. Loss of THF might facilitate this reorientation by relieving some of the steric congestion; however, THF expulsion in solution is not observed, nor is THF lost under vacuum (10^{-5} Torr, 25 °C).

In the analogous triphenylphosphine system, no reaction occurs between $ReH_5(PPh_3)_3$ and $Cp_2LnMe(THF)$ at room temperature in benzene solvent over 48 h. Heating to 85 °C in toluene leads to partial (50%) formation of $Cp_2Y(THF)(H)_4Re(PPh_3)_3$ after 3 h. Prolonged heating or higher temperatures lead to decomposition.

Molecular Structure of $Cp_2Y(THF)(H)_4Re(PMe_2Ph)_3$, 2. The X-ray crystallographic study revealed a bimetallic structure which contained an average Re–Y distance, 3.110 (5) Å, similar to that of **1** (Figure 4). Selected bond distances and angles are given in Table III. The coordination environment about yttrium in **2** is difficult to directly compare with **1** and with $[(MeC_5H_4)_2Y(\mu\text{-}H)(THF)]_2$ since the hydride ligands were not located. However, the O–Y–(Cp centroid) angles of 98.2 and 101.3° are similar to those of **1** (99.9 and 102.2°). The most notable differences in these molecules is the very small cent–Y–cent angle of 119.3° in $Cp_2Y(THF)(H)_4Re(PMe_2Ph)_3$ versus 123.0° for $Cp_2Y(THF)(\mu\text{-}H)_2ReH_4(PPh_3)_2$. It is evident that the addition of another phosphine ligand forces the rings to bend further back. As in **1**, THF is retained (Y–O = 2.36 (21) Å) despite steric crowding.

In contrast to **1**, steric crowding is evident to a much lesser degree in the rhenium portion of the molecule. Here the averages of the small P–Re–P angles are 92.1 (3) and 95.6 (3)°, while the large P–Re–P angle averages 127.1 (3)°. These values are similar to 92.9 (0), 96.6 (0), and 135.5 (0)° found for the $ReH_4(PPh_2Me)_3$ fragment in $ReH_4(PPh_2Me)_3AlMe_2$[28] but are smaller than the angles of 99.8 (2), 101.9 (2), and 149.5 (2)° found in $ReH_5(PMe_2Ph)_3$.[8] The larger angles in the rhenium–aluminum complex may be due to the steric crowding caused by the larger PPh_2Me ligand.

The configuration around rhenium in $ReH_4(PPh_2Me)_3AlMe_2$ was determined by X-ray crystallography to be a pentagonal bipyramid. Given the angular similarity between this complex and **2**, a reasonable coordination environment for **2** also involves a pentagonal bipyramid in which two phosphorus atoms (P(1) and P(2)) lie in the equatorial (pentagonal) plane that contains rhenium and the other (P(3)) lies above the plane. The bridging hydride ligands would also lie in the equatorial plane. Consistent with this configuration, the P(3)–Re–P(1) and P(3)–Re–P(2) angles are found to be near 90°. The observed P(1)–Re–P(2) angle of 127° is smaller than the expected 144°; however, this may be due to steric interaction with the THF ligand. In agreement with the proposed geometry, the Y–Re–P(1) and Y–Re–P(2) angles of 105.8 (2) and 112.4 (2)° are close to the idealized 108°. The larger Y–Re–P(2) angle is reasonable since P(2) lies on the same side of the molecule as the THF ligand. The Y–Re–P(3) angle of 123.4 (2)° is much larger than the expected 90° in the idealized geometry. However, the openness of this angle may be attributed to steric interaction with the C_5H_5 ring. Hence, the bending back of ligands on both yttrium and rhenium appear to relieve potentially unfavorable steric crowding.

Synthesis of $Cp_2Y(THF)Re_2H_7(PMe_2Ph)_4$. $Cp_2LnMe(THF)$ complexes also react with bimetallic rhenium polyhydrides.[2] $Cp_2YMe(THF)$ reacts with $Re_2H_8(PMe_2Ph)_4$ in THF at 25 °C to generate methane (identified by ^1H NMR) and $Cp_2Y(THF)Re_2H_7(PMe_2Ph)_4$ (eq 4). The ^1H NMR (C_6D_6, 25 °C) spectrum

$$Cp_2YMe(THF) + Re_2H_8(PMe_2Ph)_4 \rightarrow Cp_2Y(THF)Re_2H_7(PMe_2Ph)_4 + CH_4 \quad (4)$$

of this compound shows signals characteristic of bound THF along with one C_5H_5 resonance and one broad hydride resonance. The presence of only one hydride resonance can be attributed to rapid fluxionality of the hydride ligands about rhenium and yttrium. When the toluene-d_8 sample is cooled to –60 °C, this resonance broadens into the baseline, but no new resonances were resolved before the solvent froze. The $\{^1H\}^{31}P$ NMR spectrum shows one singlet resonance. These data are consistent with the presence of a highly symmetrical molecule or the oversimplification of the spectrum by dynamic averaging process.

Molecular Structure of $Cp_2Y(THF)Re_2H_7(PMe_2Ph)_4$, 3. An X-ray crystallographic study revealed a highly unsymmetrical trimetallic structure for **3** (Figure 5). Selected bond angles and distances for $Cp_2Y(THF)Re_2H_7(PMe_2Ph)_4$ are given in Table IV. The molecule has an open triangular or L-shaped form where the Y–Re(1)–Re(2) angle is 94.8 (1)°. This orientation renders the rhenium and phosphorus centers inequivalent. The 4.186-Å Re(2)–Y(1) distance is clearly beyond the range of significant interaction. The 3.090 (2)-Å Re(1)–Y(1) distance is similar to Re–Y distances in **1** and **2** and is reasonable for a hydride-bridged linkage. Although the hydrides were not located from the X-ray diffraction data, a structure in which two hydrides connect yttrium and Re(1) is proposed. It is interesting to note that the 2.576 (1)-Å Re–Re distance in **3** is similar to the 2.538 (4)-Å Re–Re distance in $Re_2H_8(PEt_2Ph)_4$.[29] Hence, replacement of a proton in $Re_2H_8(PMe_2Ph)_4$ by a $Cp_2Y(THF)^+$ moiety has little effect

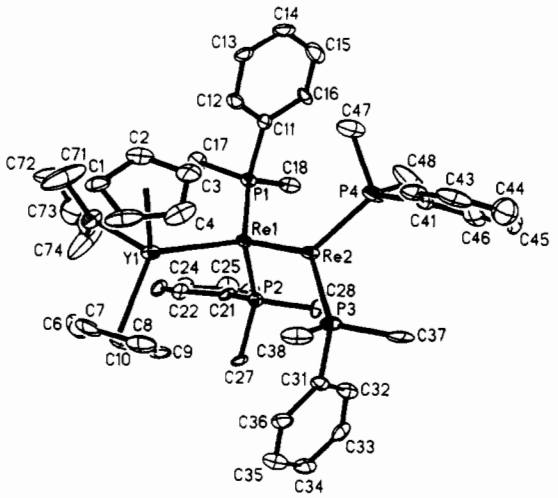

Figure 5. ORTEP drawing (30% level) of non-hydrogen atoms of $Cp_2Y(THF)Re_2H_7(PMe_2Ph)_4$, **3**. Carbon atom labels are omitted for clarity.

Table IV. Selected Bond Distances (Å) and Angles (deg) for $Cp_2Y(THF)Re_2H_7(PMe_2Ph)_4$, **3**[a]

Interatomic Distances (Å) with Esd's			
Re(1)–Re(2)	2.576 (1)	Re(1)–Y(1)	3.090 (2)
Re(1)–P(1)	2.315 (3)	Re(1)–P(2)	2.356 (4)
Re(2)–P(3)	2.308 (4)	Re(2)–P(4)	2.295 (4)
Y(1)–O(1)	2.405 (11)	Y(1)–C(1)	2.724 (17)
Y(1)–C(2)	2.701 (16)	Y(1)–C(3)	2.668 (16)
Y(1)–C(4)	1.635 (20)	Y(1)–C(5)	2.710 (23)
Y(1)–C(6)	2.751 (19)	Y(1)–C(7)	2.714 (19)
Y(1)–C(8)	2.671 (18)	Y(1)–C(9)	2.647 (15)
Y(1)–C(10)	2.679 (14)	Y(1)–Cent(1)	2.411
Y(1)–Cent(2)	2.423		
Interatomic Angles (deg) with Esd's			
Re(2)–Re(1)–Y(1)	94.8 (1)	Re(2)–Re(1)–P(1)	122.0 (1)
Y(1)–Re(1)–P(1)	121.3 (1)	Re(2)–Re(1)–P(2)	108.2 (1)
Y(1)–Re(1)–P(2)	117.1 (1)	P(1)–Re(1)–P(2)	94.4 (1)
Re(1)–Re(2)–P(3)	130.9 (1)	Re(1)–Re(2)–P(4)	123.2 (1)
P(3)–Re(2)–P(4)	105.4 (1)	Re(1)–Y(1)–O(1)	98.1 (3)
Re(1)–Y(1)–Cent(1)	112.8	Re(1)–Y(1)–Cent(2)	116.3
Cent(1)–Y(1)–O(1)	101.4	Cent(2)–Y(1)–O(1)	100.2
Cent(1)–Y(1)–Cent(2)	122.1		
Y(1)–O(1)–C(71)	130.8 (12)	Y(1)–O(1)–C(74)	122.8 (13)
C(71)–O(1)–C(74)	106.2 (17)	O(1)–C(71)–C(72)	97.6 (22)
C(71)–C(72)–C(73)	112.7 (23)	C(72)–C(73)–C(74)	101.9 (26)
O(1)–C(74)–C(73)	115.6 (28)		

[a] Cent(1) is the centroid of the C(1)–C(5) ring. Cent(2) is the centroid of the C(6)–C(10) ring.

on the Re–Re distance (despite a formal oxidation state change of Re^{IV} to Re^{III}). A similar result was observed in $Re_2H_6(Au(PPh_3))_2(PMe_2Ph)_4$ and $Re_2H_7Au(PPh_3)(PPh_3)_4$, which have Re–Re distances of 2.5644 (10) and 2.571 (1) Å, respectively.[30,31] Hence, the isolobal analogy[32] between "$(PPh_3)Au^+$" and a proton may be extendable to a "Cp_2Y^+" unit. Theoretical calculations have led to a similar argument for "$[Me_3SiC_5H_4]_2Nb^+$" in $[(Me_3SiC_5H_4)_2NbAuH_2]_3$.[33]

The positions of the phosphine ligands in **3** are substantially different from those in $Re_2H_8(PEt_2Ph)_4$, where, in the latter complex, the four phosphorus atoms are nearly coplanar and the P–Re–P angles are 102.7 (1)°. The phosphine ligands nearest to the $Cp_2Y(THF)$ moiety in **3** have a P(1)–Re(1)–P(2) angle

(28) Skupinski, W. A.; Huffman, J. C.; Bruno, J. W.; Caulton, K. G. *J. Am. Chem. Soc.* **1984**, *106*, 8128.
(29) Bau, R.; Carroll, W. E.; Teller, R. G.; Koetzle, T. F. *J. Am. Chem. Soc.* **1977**, *99*, 3872–3874.
(30) Sutherland, B. R.; Ho, D. M.; Huffman, J. C.; Caulton, K. G. *Angew. Chem., Int. Ed. Engl.* **1987**, *26*, 135–137.
(31) Moehring, G. A.; Fanwick, P. E.; Walton, R. A. *Inorg. Chem.* **1987**, *26*, 1861–1866.
(32) Lauher, J. W.; Hoffman, R. *J. Am. Chem. Soc.* **1976**, *98*, 1729–1742.
(33) Antinolo, A.; Burdett, J. K.; Chaudret, B.; Eisenstein, O.; Fajardo, M.; Jalon, F.; Lahoz, F.; Lopez, J. A.; Otero, A. *J. Chem. Soc., Chem. Commun.* **1990**, 17–19.

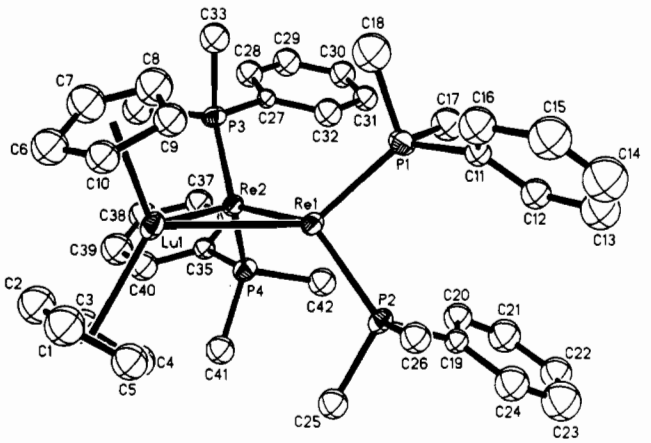

Figure 6. ORTEP drawing (40% level) of the non-hydrogen atoms of $Cp_2LuRe_2H_7(PMe_2Ph)_4$, **4**. Carbon atom labels are omitted for clarity.

of 94.4 (1)°, while those on the other side of the molecule have a P(3)–Re–P(4) angle of 105.4 (1)°. These differences can be attributed to steric crowding between the phosphines and the $Cp_2Y(THF)$ moiety. The Re(2)–Re(1)–P(1) angle of 122.0 (1)° and Re(2)–Re(1)–P(2) angle of 108.2 (1)° in **3** also differ from the analogous 129.2 (1) and 128.0 (1)° angles in $Re_2H_8(PEt_2Ph)_4$. Steric congestion is also noted in the yttrium coordination environment, where a (ring centroid)–Y–(ring centroid) angle of 122.1° is observed. Except for the 119.3° angle in **2**, this angle is smaller than any previously reported for Cp_2Y systems (cf. 125.5° in $Cp_2Y(CH_2SiMe_3)_2^-$).[25]

Synthesis of $Cp_2LuRe_2H_7(PMe_2Ph)_4$. When the same synthetic and product isolation procedures used for $Cp_2Y(THF)Re_2H_7(PMe_2Ph)_4$ are applied to the reaction of $Cp_2LuMe(THF)$ with $Re_2H_8(PMe_2Ph)_4$ in THF, the product isolated was found to be free of THF by ^1H NMR spectroscopy (eq 5). The NMR patterns of this $Cp_2LuRe_2H_7(PMe_2Ph)_4$ complex are analogous to those of $Cp_2Y(THF)Re_2H_7(PMe_2Ph)_4$, except that the absence of THF leads to a more symmetrical compound (see below).

$$Cp_2LuMe(THF) + Re_2H_8(PMe_2Ph)_4 \rightarrow Cp_2LuRe_2H_7(PMe_2Ph)_4 + CH_4 + THF \quad (5)$$

Molecular Structure of $Cp_2LuRe_2H_7(PMe_2Ph)_4$, 4. In contrast to **3**, the X-ray study of **4** revealed a symmetrical trimetallic complex (Figure 6). Selected bond angles and distances are given in Table V. With THF absent, the three metals of $Cp_2LuRe_2H_7(PMe_2Ph)_4$ adopt a closed triangular shape with idealized C_{2v} symmetry. This configuration renders the phosphorus nuclei symmetry-equivalent, and both rhenium atoms are equidistant from lutetium. The metal–metal distances, Re(1)–Lu = 3.068 (1) and Re(2)–Lu = 3.025 (1) Å, are slightly smaller than those in **1**–**3**, which is consistent with the fact that Lu^{3+} is 0.042 Å smaller than Y^{3+}.[24] While hydride ligands were not located from the X-ray data, the similarities in the two Re–Lu distances imply a symmetrical disposition of bridging hydride ligands about the Re_2Lu unit. Two μ_2-hydride bridges and possibly a μ_3-hydride ligand[34] are likely to connect lutetium to the rhenium atoms. As in **3**, the Re–Re distance of 2.561 (1) Å for **4** is similar to the Re–Re distance in $Re_2H_8(PEt_2Ph)_2$.[29]

The positions of the phosphine ligands in **4** are different from those in $Re_2H_8(PEt_2Ph)_4$ and **3**. Smaller P–Re–P angles of 95.2 (2) and 94.0 (2)° are found, which indicates that the steric environments about both rhenium centers are influenced by the Cp_2Lu moiety. The 117.6 (1)° Re(2)–Re(1)–P(1) and 118.9 (1)° Re(1)–Re(2)–P(4) angles are smaller than those of Re(2)–Re(1)–P(2), 130.9 (1)°, and Re(1)–Re(2)–P(3), 130.6 (1)°, the latter of which are similar to those found for $Re_2H_8(PEt_2Ph)_4$. This correlates with a subtle twist of the Cp_2Lu fragment in a direction that results in closer interactions between the cyclopentadienyl ring and the P(1) and P(4) phosphine ligands. The (ring centroid)–Lu–(ring centroid) angle in **4** is 124.2°.

Table V. Selected Bond Distances (Å) and Angles (deg) for $Cp_2LuRe_2H_7(PMe_2Ph)_4$[a]

Interatomic Distances (Å) with Esd's			
Re(1)–Re(2)	2.561 (1)	Re(1)–Lu(1)	3.068 (1)
Re(1)–P(1)	2.337 (5)	Re(1)–P(2)	2.319 (4)
Re(2)–Lu(1)	3.025 (1)	Re(2)–P(3)	2.320 (5)
Re(2)–P(4)	2.335 (5)	Lu(1)–C(1)	2.619 (23)
Lu(1)–C(2)	2.602 (22)	Lu(1)–C(3)	2.641 (21)
Lu(1)–C(4)	2.652 (20)	Lu(1)–C(5)	2.648 (21)
Lu(1)–C(6)	2.592 (20)	Lu(1)–C(7)	2.603 (22)
Lu(1)–C(8)	2.641 (21)	Lu(1)–C(9)	2.629 (19)
Lu(1)–C(10)	2.643 (18)	Lu(1)–C(9)	2.351
Lu(1)–Cent(2)	2.325		

Interatomic Angles (deg) with Esd's			
Re(2)–Re(1)–Lu(1)	64.3 (1)	Re(2)–Re(1)–P(1)	117.6 (1)
Lu(1)–Re(1)–P(1)	133.5 (1)	Re(2)–Re(1)–P(2)	130.9 (1)
Lu(1)–Re(1)–P(2)	118.3 (1)	P(1)–Re(1)–P(2)	95.2 (2)
Re(1)–Re(2)–Lu(1)	66.0 (1)	Re(1)–Re(2)–P(3)	130.6 (1)
Lu(1)–Re(2)–P(3)	119.7 (1)	Re(1)–Re(2)–P(4)	118.9 (1)
Lu(1)–Re(2)–P(4)	131.2 (1)	P(3)–Re(2)–P(4)	94.0 (2)
Re(1)–Lu(1)–Re(2)	49.7 (1)	Re(1)–Lu(1)–Cent(1)	119.3
Re(1)–Lu(1)–Cent(2)	110.9	Re(2)–Lu(1)–Cent(1)	112.5
Re(1)–Lu(1)–Cent(2)	118.1	Cent(1)–Lu(1)–Cent(2)	124.2

[a] Cent(1) is the centroid of the C(1)–C(5) ring. Cent(2) is the centroid of the C(6)–C(10) ring.

Solution Behavior of 3 and 4. When a toluene-d_8 sample of **3** is heated to 65 °C, the broad hydride resonance sharpens into a multiplet arising from ^{31}P and ^{89}Y coupling. Phosphorus decoupling yields a doublet (J_{Y-H} = 7.2 Hz), which precludes dissociation into the solvent-separated ion pair $[Cp_2Y(THF)]^+[Re_2H_7P_4]^-$ as being responsible for the dynamic process which averages the ^{31}P NMR signals. Moreover, the observed coupling is additional evidence for the existence of bridging hydride ligands. The magnitude of this ^{89}Y–^1H coupling constant falls in line with those observed for **1**, 8.3 Hz, and **2**, 14.7 Hz, such that, as the percentage of terminal hydride ligands increases, the observed coupling constant decreases. The fluxionality of the hydride ligands about the three metals in **3** appears to give an averaged coupling constant at 65 °C. At 80 °C, however, the ^{31}P-decoupled ^1H NMR hydride resonance becomes a singlet; i.e., ^{89}Y–^1H coupling is absent. Recooling the sample and recording the spectrum shows no indication of decomposition. Apparently at 80 °C, a dissociative process occurs.

The lutetium structure provides an attractive intermediate for the fluxional process which averages the ^{31}P NMR signals of $Cp_2Y(THF)Re_2H_7(PMe_2Ph)_4$. Exchange involving intramolecular migration of PMe_2Ph is less likely since the implied μ_2-bridging phosphine is an unknown bonding mode. A dynamic process that involves dissociation of THF is shown in eq 6.

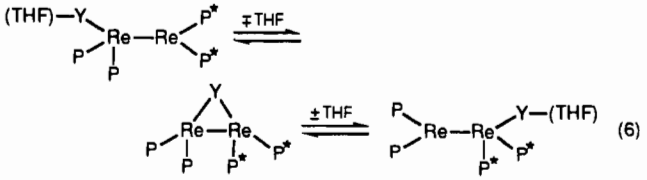

(6)

Consistent with this hypothesis, the dynamic process can be slowed by lowering the temperature. The $^{31}P\{^1H\}$ NMR spectrum of **3** at −88 °C in 1:3 toluene/THF shows two resonances too broad to permit resolution of ^{31}P–^{31}P coupling. These resonances correspond to the two pairs of inequivalent phosphorus atoms that are found in the solid state. A more significant feature observed in this spectrum is an additional singlet which corresponds

(34) Cf: (a) Evans, W. J.; Meadows, J. H.; Hanusa, T. P. *J. Am. Chem. Soc.* **1984**, *106*, 4454–4460. (b) Evans, W. J.; Sollberger, M. S.; Khan, S. I.; Bau, R. *J. Am. Chem. Soc.* **1988**, *110*, 439–446.

to the THF-*free* complex $Cp_2YRe_2H_7(PMe_2Ph)_4$ observed in an amount equal to that of **3**. In the absence of added THF, this decoalescence is not observed. In toluene-d_8 at 25 °C, the THF ^1H chemical shifts of **3** are very close to those of free THF suggesting that **3** is significantly solvated only in the presence of excess THF. The dynamic process shown in eq 6 also suggests that rapid exchange between free and coordinated THF should take place. The ^1H NMR of **3** in THF-d_8 only shows resonances that correspond to free proteo-THF. The coordinated THF has been completely equilibrated with the THF-d_8 in the time required to obtain the spectrum. Dissolving **3** in toluene, followed by removal of solvent in vacuo, yields the THF-free yttrium species $Cp_2YRe_2H_7(PMe_2Ph)_4$. When dissolved in THF, this complex is readily resolvated and, hence, contains latent unsaturation.

In contrast to the yttrium system, where products with and without coordinated THF are accessible, treatment of $Cp_2LuRe_2H_7(PMe_2Ph)_4$ with 1 equiv of THF in C_6D_6 gives no spectral shifts. Resonances corresponding to free THF appear, and no evidence for THF binding is observed. The marginally smaller radius of lutetium (0.848 vs 0.88 Å for yttrium)[24] may cause this difference in chemical behavior. A similar difference in chemical behavior has been observed for hydrogenation reactions of $[Cp_2YMe]_2$ and $[Cp_2LuMe]_2$.[35,36]

These results suggest that the $Cp_2LnRe_2H_7(PMe_2Ph)_4$ complexes may be capable of size-selective binding. Substrates smaller than THF may add to the lutetium complex without reverting to homometallic constituents. When THF is lost from the yttrium complex, the vacant coordination position is filled by a hydride ligand, with concomitant conversion of the open L-shaped form to a closed metal triangle. The reverse occurs on addition of THF. Hence, selective polymetallic chemistry may be achievable with complexes of this class.

Reactivity. The reactivity of $Cp_2Y(THF)H_6Re(PPh_3)_2$ with CO and CO_2 was initially examined to see if any hydride ligands in **1** could be transferred to these substrates. No reaction was observed with either of these substrates at two atmospheres up to the decomposition temperature of **1**, ~70 °C. Diphenylacetylene was also found to be unreactive. **1** does react with 2 atm of ethylene to form several metal-containing products as well as low molecular weight olefin oligomers characterized by ^1H NMR and mass spectroscopy. The rhenium hydride side products $Re_2H_8(PPh_3)_4$, $Re_5H_5(PPh_3)_3$, and $CpReH_2(PPh_3)_2$ were identified by ^1H and $\{^1H\}^{31}P$ NMR spectroscopy.[6,20,37,38] The stoichiometric reaction of ethylene with **1** at −78 °C was found to give similar products in lower yield and approximately 50% of unreacted **1**. Since a molar quantity of ethylene is consumed by less than an equimolar amount of **1**, the initial ethylene reaction product displays greater reactivity toward ethylene than does **1** under these reaction conditions.

Complex **1** also reacts with two atmospheres of propylene in both toluene and THF to form oligomers and the same rhenium phosphine hydride byproducts observed in the ethylene reaction. Reaction of **1** with styrene gave analogous results. The hydrogenation product ethyl benzene is also observed in the ^1H NMR spectrum. It should be noted that neither $ReH_6(PPh_3)_2^-$ [16] nor $(C_5Me_5)_2Sm(THF)_2^+$,[39] which are models of the components of **1**, react with ethylene. Hence, the reactivity of **1** with ethylene demonstrates that the heterometallic system can achieve reactions not possible with the individual components.

Reactions of $Cp_2LnRe_2H_7(PMe_2Ph)_4$. In sharp contrast to the reactivity of **1**, $Cp_2YRe_2H_7(PMe_2Ph)_4$ was found to be unreactive toward ethylene in both toluene and THF. In further contrast, **3** reacts under 2 atm of CO in toluene to form a complicated mixture of products. A similar result is observed when CO is added stoichiometrically. The ^1H NMR of these products reveals triplet hydride resonances. This implies that reaction is taking place at the dirhenium portion of the molecule, where the Re–Re multiple bond is cleaved. The presence of only one rhenium in $Cp_2Y(THF)H_6Re(PPh_3)_2$ may account for its nonreactivity with CO. Both $Cp_2LnRe_2H_7(PMe_2Ph)_4$ complexes, **3** and **4**, were also found to be highly reactive with CO_2 in toluene and THF, giving both soluble and insoluble products. Although ^1H NMR and IR spectroscopic analysis of the soluble product showed the presence of hydride, phosphine, and C–O containing functionalities, the data were not structurally definitive. X-ray-quality crystals of the product have not yet been obtained.

Conclusion

The reaction between rhenium phosphine polyhydrides and cyclopentadienyllanthanide and -yttrium alkyl complexes has proven to be a good general method to make heterometallic complexes containing reactive ligands. As anticipated, hydride ligands are effective in bringing these metals close together in reactive complexes. Variations in structure and bonding of the heterometallic products can be as extensive as are found in the individual components, and the heterometallic products display reactivity beyond that known for the individual constituents. Interestingly, the hydride chemical shifts of the heterometallic species reported here resemble those of the parent rhenium polyhydrides (negative δ values) and lack the positive chemical shifts found for some lanthanide hydrides.[34] The metal skeletal isomerization observed for the Re_2Ln species is an example of an uncommon but currently interesting phenomenon.[40] It appears that such rearrangement is possible for the heterometallic species reported here due to the versatile bonding potential of the hydride ligand: labile ligand loss is compensated by terminal-to-bridging hydride conversion, which, in turn, alters the multimetal polyhedral form. The selective THF bonding and variable reactivity depending on substrate and polymetallic complexes of this type will require careful control of steric factors (primarily on the lanthanide and yttrium side) and electronic factors (primarily on the rhenium side) within the synthetic boundaries for the formation of these species.

Acknowledgment. This work was supported by grants from the National Science Foundation (to K.G.C.) and the Division of Chemical Sciences of the Office of Basic Energy Sciences of the Department of Energy (to W.J.E.). Funds for the purchase of the X-ray equipment were made available from NSF Grant CHE-85-14495. We thank Rhenium Alloys for material support.

Supplementary Material Available: Tables of crystal data, positional parameters, bond distances, bond angles, and thermal parameters for **1**, **2**, and **4** (45 pages). Ordering information is given on any current masthead page.

Registry No. **1**, 144564-83-0; **2**, 144564-84-1; **3**, 144564-85-2; **4**, 144564-86-3; $ReH_7(PPh_3)_2$, 12103-40-1; $Cp_2YMe(THF)$, 128190-94-3; $Cp_2Lu(THF)H_6Re(PPh_3)_2$, 144564-87-4; $Cp_2Lu(THF)H_4Re(PMe_2Ph)_3$, 144564-88-5; $Cp_2Y(THF)H_4Re(PPh_3)_3$, 144564-89-6; $Re_2H_8(PMe_2Ph)_4$, 76317-34-5; $Cp_2LuMe(THF)$, 76207-05-1; $[Cp_2LuMe]_2$, 99583-15-0; $Cp_2YRe_2H_7(PMe_2Ph)_4$, 144564-90-9; $[Cp_2YMe]_2$, 60997-40-2; $ReH_5(PPh_3)_3$, 12103-36-5; $ReH_5(PMe_2PH)_3$, 58513-89-6.

(35) Evans, W. J.; Dominguez, R.; Hanusa, T. P. *Organometallics* **1986**, *5*, 263–270.
(36) Evans, W. J. *Polyhedron* **1987**, *6*, 803–835.
(37) Baudry, D.; Ephritikhine, M. *J. Chem. Soc., Chem. Commun.* **1980**, 249.
(38) Baudry, D.; Ephritikhine, M.; Felkin, H. *J. Organomet. Chem.* **1982**, *224*, 363–376.
(39) Evans, W. J.; Ulibarri, T. A.; Chamberlain, L. R.; Ziller, J. W.; Alvarez, D. *Organometallics* **1990**, *9*, 2124–2130.
(40) For a brief review of skeletal isomerization of transition metal clusters, see: Braunstein, P.; de Meric de Bellefon, C.; Bouaoud, S.; Grandjean, D.; Halet, J.-F.; Saillard, J.-Y. *J. Am. Chem. Soc.* **1991**, *113*, 5282.